Memoirs of the School of Engineering, Nagoya University
Vol.45, No.2 (1993)

NUMERICAL SIMULATION OF PLUME IMPINGEMENT ON THE LUNAR SURFACE

Takeo SOGA, Byung Gon KIM*, and Satoshi KOGURE**

Department of Aeronautical Engineering

(Received November 11, 1993)

Abstract

Impingement of axisymmetric free jet from a supersonic nozzle (M_e=5) into a vacuum on a plate was studied based upon the Direct Simulation Monte Carlo method for hard sphere molecules. The distance from the nozzle exit to the plate was four times of the nozzle diameter. Plume envelopment due to plume impingement was found as the previous study based upon the continuum flow theory. Obtained results for the nozzle Knudsen number $Kn_D = 0.00625$ showed a good agreement with the results of PLM. The maximum shear stress on the flat plate is found at $R/D \approx 0.7$ for the case of $Kn_D = 0.00625$.

1. Introduction

Plume impingement on a perpendicular surface in a vacuum environment takes place during the landing of spacecrafts on the lunar surface, during the docking of spacecrafts, and so on. In the 1960's this problem was investigated theoretically and experimentary[1)-6)] from the necessity for the Apollo mission. Roberts[5)] investigated the impingement of a single jet on a dust-covered lunar surface and has found that the worst erosion and greatest loss of visibility will take place at a height of less than about 20 feet.

However, there are less studies for the case of small nozzle-plate separation and more detailed studies on this problem are now required. This paper aims to reveal effects of rarefaction on the plume impingement through the direct simulation of the Boltzmann equation[7)-9)] and to examine the previous results obtained using the Piecewise Linear Method (PLM)[10)]. Plume impingement of an axisymmetric free jet issuing from a supersonic parallel nozzle on a perpendicular flat plate in a vacuum environment is treated in this paper. Results of the numerical simulation for the smallest Knudsen number will span with the results of continuum flow.

---

* Graduate student

**Present address; Tukuba space center, National space development agency, Tukuba

2. Calculation Procedure

Monte Carlo simulations of plume impingements in a vacuum environment are executed in this paper. The axisymmetric flow field is divided into coaxial annular disks (cells) with the thickness ΔZ and the width ΔR where the radius of the inner and the outer cylinders are $(N-1) \times \Delta R$ and $N \times \Delta R$, respectively. Three dimensional motions of molecules in each cell are projected on a rectangular (two-dimensional) plane, $(N-1) \times \Delta R \leq R \leq N \times \Delta R$ and $(M-1) \times \Delta Z \leq Z \leq M \times \Delta Z$. Molecules pass through the axis of symmetry are, thus, suffer specular reflection at R=0 on the two-dimensional plane.

A schematic drawing of the calculation domain, $R_{max} = 5D$ and $Z_{max} = 4D$, is shown in Fig. 1. The nozzle lip has the thickness D/4. In the case of free expansion flows without a plate, the domain of simulation is slightly extended backward $(-D/8 \leq Z \leq 0)$. Molecules are supplied through additional cells just inside the nozzle exit. The number of molecules feeded in the smallest cell including the nozzle axis is changed from 10 to 20.

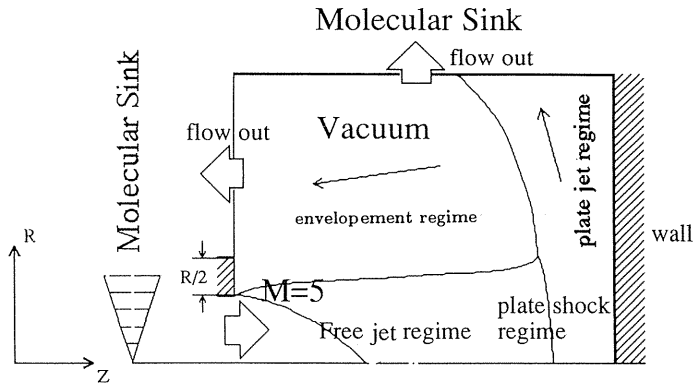

Fig. 1. Coordinates system, calculation region, and boundary conditions.

Boundaries and boundary conditions of the calculation region are given in (a) to (e).

(a) Supersonic nozzle: One additional array of cells are provided in the inside of the nozzle and the number of molecules in each additional cell is kept constant. Velocities of gas molecules obey Maxwellian distribution pertinent to a nozzle exit condition. Pressure P_e, temperature T_e, and number density n_e of the nozzle exit are given as the isentropic values for the nozzle exit Mach number M_e. Molecules move to the next cells in the domain of simulation by random walks.

(b) Nozzle lip and Outer surface: molecules impinged on the nozzle lip and on the outer surface of the nozzle suffer diffuse reflection.

(c) Flat plate: Molecules impinged on the solid flat plate perpendicular to the axis of free jet suffer specular reflection or diffuse reflection. In the case of diffuse reflection, we assume that the temperature of the solid boundaries is same as T_e.

(d) Axisymmetric line: Molecules impinge on the axisymmetric line suffer specular reflection.

(e) Boundaries of the simulated domain: These boundaries act as molecular sink, i.e., no molecules enter into the simulated domain through these surfaces (see Fig. 1).

Table 1. Values of parameters used in the simulation

case	flow type	Kn number	Molecule numbers (base cell)	cell size $(Z\times R)\lambda_e$	sampling number	Cpu times
1	Free jet	0.00625	20	4.0× 4.0	1,500,000	140
2	Impingement	0.1	10	1.0× 1.0	245,000	12
3	Impingement	0.05	10	1.0× 1.0	402,000	30
4	Impingement	0.05 *	10	1.0× 1.0	421,000	34
5	Impingement	0.025	10	1.0× 1.0	823,000	110
6	Impingement	0.0125	15	2.0× 2.0	1,600,000	160
7	Impingement	0.00625	20	4.0× 4.0	1,800,000	172
8	Impingement	0.00625*	20	4.0× 4.0	2,211,000	220

CPU times indicates minutes. * denote diffuse reflection with flat plate. In the case of diffuse reflection, the plate temperature is same as the temperature of nozzle exit in order to compare with the inviscid continuum results[10].

Simulation is carried out employing the hard sphere molecules. Molecules are initially issuing from the nozzle into a vacuum environment by the random walks. The Knudsen numbers Kn_D defined by $\mathrm{Kn}_D = \lambda_e/D$ where λ_e denotes the mean free path pertinent to the flow at the nozzle exit are shown in Table 1.

The time step Δt_m for which molecules take collisionless motions is chosen as 1/30 of the mean free time. Molecules in the cell after each ten time increments $10 \times \Delta t_m$ are taken as sample molecules. The sampling of molecules is started appropriately when the number of molecules in the calculation domain becomes nearly constant.

Cell sizes employed in the present simulation are listed in Table 1. For a small Knudsen number, a large cell size is used. If the cell size (ΔZ or ΔR) exceeds the local mean free path, obtained results may be close to the results of Euler equation[10]. In the case of diffuse reflection, finer cells ($0.5\lambda_e \times 0.5\lambda_e$) are provided adjacent to the plate surface.

Extending the Boyd's[11] technique to the Null Collision scheme[9], simulation scheme is vectorized to 99.9 percents (FACOM, VP200).

3. Results and Discussion

Numerical simulation was carried out for the case when the uniform parallel free jet issuing from a supersonic nozzle into a vacuum impinges vertically on a flat plate located downstream of the free jet. The exit Mach number M_e was set $M_e = 5$ and the distance from the nozzle exit to the plate was chosen as $Z = 4D$. The results are presented in nondimensional forms where pressures, temperature and distance are normalized by P_e, T_e, and D, respectively. Key parameters of the simulation are shown in Table 1.

3. 1. Free jet into a vacuum

Fig. 2 shows the free expansion flow from a supersonic nozzle into a vacuum without plate. Expansion angle is about 40°. In Fig. 3 is compared the Mach number along the axis of free jet with the results of PLM[10] and experiments[1),2)]: the experimental data were obtained using a converging-divering conical nozzle with θ=15°, $P_0/P_\infty = 250\times10^3$, and M_e=4.79

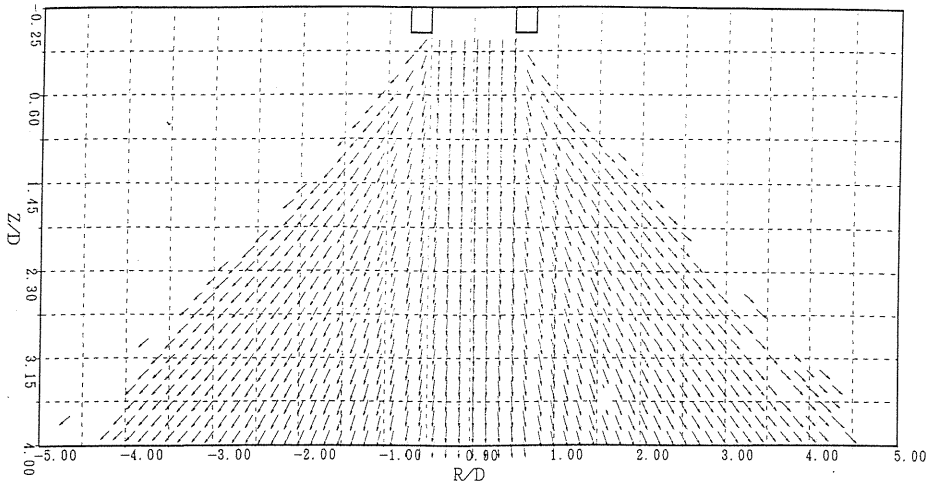

Fig. 2. Velocity vectors in the free expansion flow from supersonic nozzle (M_e=5); $Kn_D = 0.00625$.

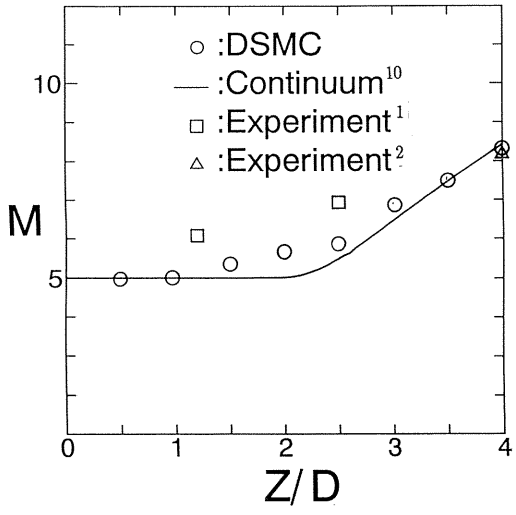

Fig. 3. Mach number distribution along the line of symmetry of expansion flow from supersonic nozzle (Me=5); $Kn_D = 0.00625$.

where P_0 denotes the stagnation pressure. The agreement of present results with the continuum results suggests that the present simulation can exhibit features of continuum flow to free molecular flow regimes of expansion flows.

3. 2. Plume impingement

In Fig. 4 is shown the flow field of the plume impingement (case 7 in the Table 1).

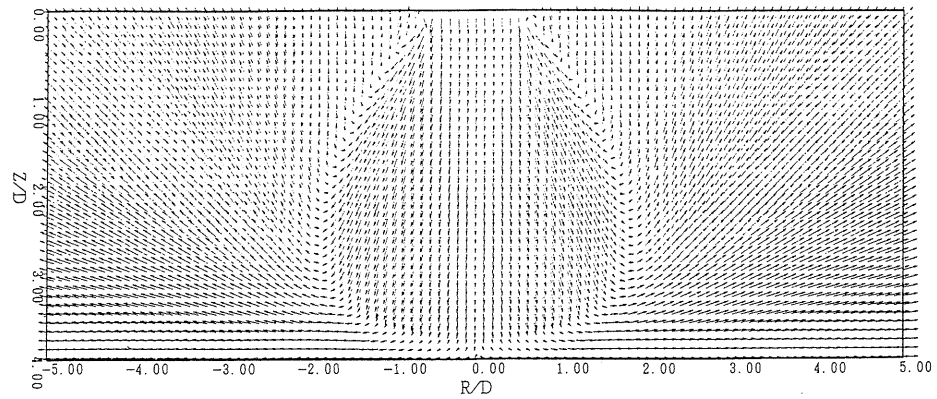

Fig. 4. Velocity vectors in the plume impingement; $Kn_D = 0.00625$ (Specular).

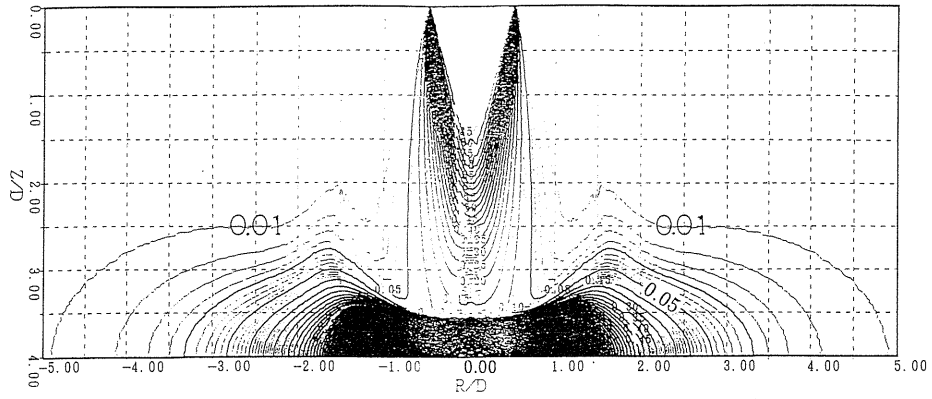

Fig. 5. Pressure contour in the plume impingement; $Kn_D = 0.00625$.

Pressure contour of this flow field is shown in Fig. 5. It is found that the flow field is composed of four regions: (1) the primary free jet upstream of a standing shock (a plate shock) (2) a plate shock through which the flow properties change suddenly, (3) a plate jet expanding radial along the plate, eventually it expands upstream, and (4) an interaction zone where the plate jet envelops the primary free jet.

(1) Primary free Jet: The expansion angle is about 31°. The decrease may be attributed to the envelopment by the plate jet. Fig. 6 illustrates Mach number contour for the case 7. A comparison with the continuum results[10] exhibits that the plate jet obtained is not so accelerated due to rarefaction effects. Present results show a qualitative agreement with the results of two dimensional plume impingements[8),12)]. It is found that the isentropic core of the primary jet is contained in the barrel and plate shocks.

(2) Plate shock: The shape of the concaved plate shock in Fig. 4 agrees well with the result of PLM[10] and shadowgraph[4]. Standoff distance of the plate shock on the axis of symmetry is shown in Fig. 7. As the Knudsen number decrease, the standoff distance approaches

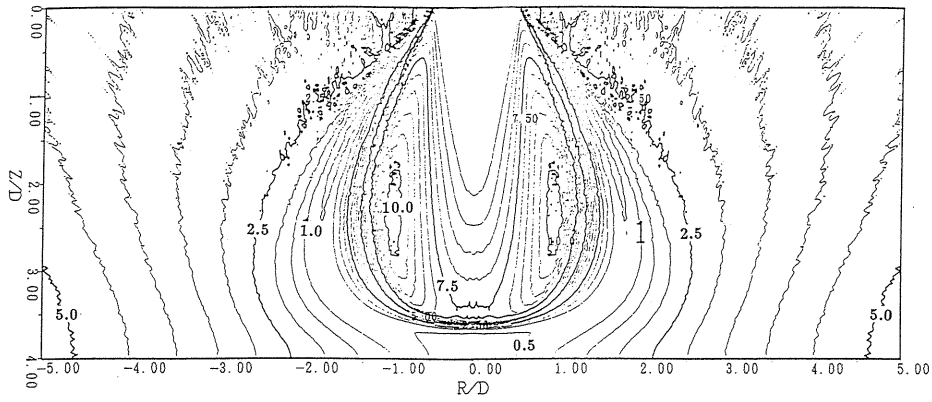

Fig. 6. Mach number contour in the plume impingement; $Kn_D = 0.00625$ (Specular).

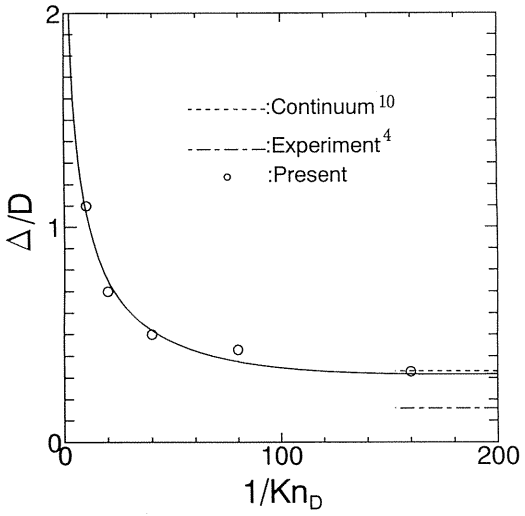

Fig. 7. Location of the plate shock along the line of symmetry vs reciprocal of Knudsen number.

the results of continuum flow[10]. But the experimental result[4] of a diatomic gas and of a diverging nozzle θ=15° yielded smaller distance than the present.

(3) The plate jet: As shown in Fig. 6, the plate jet accelerated radially to M=5.0 in the vicinity of the plate and expands toward axis (see Figs. 4 and 5). In the case of diffuse reflection, a thick boundary layer (compared with the experiments of Poreh et al.[13]) is formed in the vicinity of the plate. Thus, the plate jet is not so accelerated as the case of specular reflection. In Fig. 8 pressure distribution along the plate for various values of Kn_D are shown and are compared with the previous results[10]. The static pressures along the plate decreases rapidly as the radius increases. The stagnation pressure P_s of the case 7 is about 4% of the

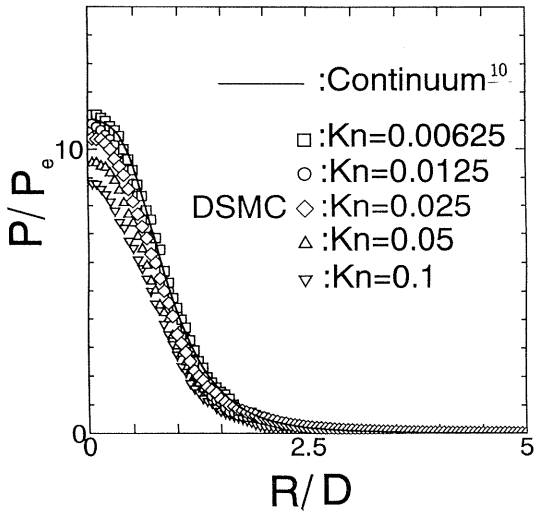

Fig. 8. Pressure distribution along the flat plate; $Kn_D = 0.00625$.

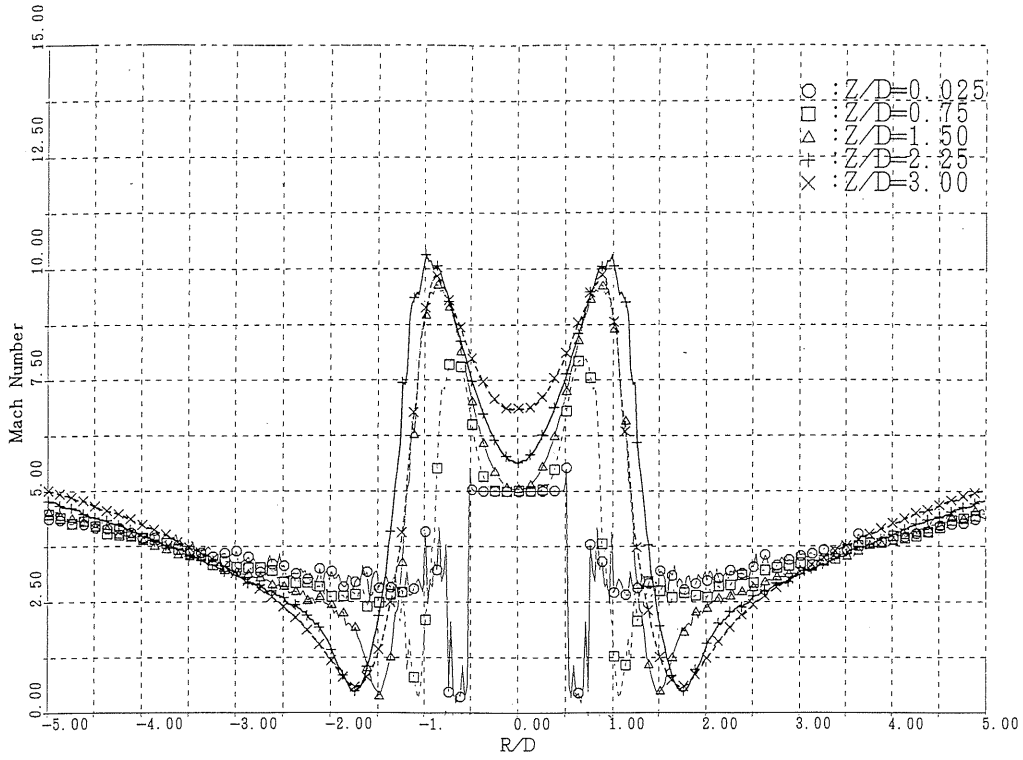

Fig. 9. Radial distribution of Mach number in the plume impingement; $Kn_D = 0.00625$.

total pressure of reservoir. Preliminary simulations for the case of diffuse reflection on the plate yielded that the maximum shear stress (case 8 in the Table 1) is created about $R/D \approx 0.7$.

(4) Plume envelopment: As is seen in Fig. 4, velocity vectors deflect abruptly at the jet boundary of the primary jet. This fact implies that the supersonic plate jet envelops the primary jet. Fig. 9 shows the radial distributions of Mach number on the planes perpendicular to the axis of symmetry. Except the case for Z/D=0.025 two supersonic branches are observed in the figure. The inner branch is the one of the primary jet; the Mach number increases through the expansion and then decreases through the barrel shock. The other branch shows an increase in the Mach number in accordance with the increase of radius; the Mach number increases through the radial expansion. The subsonic part between the two supersonic branchs denotes the shear layer where the temperature increases abruptly (figures of the temperature are not shown here). Although these interaction region is in transition regime due to rarefaction in the present simulation, these features of the plume envelopment are quite similar to the results of PLM[10].

4. Conclusions

Numerical simulation of plume impingements of free jet from a supersonic nozzle (M_e=5) into a vacuum on a flat plate located at Z=4D yielded the following conclusions: (1) The plate jet prevents the free expansion of the primary jet issuing from the supersonic nozzle. The primary jet is consequently enveloped by a strong shear layer. (2) As the Knudsen number decrease, the standoff distance of the plate shock and the pressure distribution along the flat plate approaches the inviscid continuum results without regard to choice of the boundary condition on the flat plate. The maximum value of the pressure on the plate is about 4% of the stagnation pressure of the primary jet. (3) The maximum shear stress on the flat plate is found at $R/D \approx 0.7$ for the case of $Kn_D = 0.00625$.

References

1) Vick, A.R. and Andrews, E.H., Jr.: An investigation of high underexpanded exhaust plumes impinging upon a perpendicular flat surface, 1966, NASA TN D-3269.
2) Stitt, L.E.: Interaction of highly underexpanded jets with simulated lunar surface, 1961, NASA TN D-1095.
3) Vick, A.R., Cubbage, J.M. and Andrews, E.H.Jr.: Rocket exhaust-plume problems and some recent related research, "The fluid dynamic aspects of space flight", (Gotdon and Breach, 1966), Vol.II, pp.129–180.
4) Norman, S.L. and Leonard, V.C.: Experimental investigation of jet impingement on surface of fine particles in a vacuum environment, 1965, NASA TN D-2633.
5) Roberts, L.: The interface of a rocket exhaust with the lunar surface, "The fluid dynamic aspects of space flight", (Gotdon and Breach, 1966), Vol.II, pp.269–290.
6) Eastman, D.W. and Radtke, L.P.: Flow field of an exhaust plume impinging on a simulated lunar surface, AIAA J., Vol.1 (1963), pp.1430–1431.
7) Bird, G.A.: "Molecular gas dynamics" (Clarendon Press, Oxford, 1976)
8) Nanbu, K.: Direct simulation scheme derived from Boltzmann equation. I. Mono-component gases, J. Phys. Soc. Japan, Vol.49 (1980), pp.2042–3511.

9) Koura, K.: Null-collision technique in the direct simulation Monte Carlo method, Phys. Fluids Vol.29 (1986), pp.3509–3511.
10) Kogure, S: Numerical analysis of impingement of an exhaust flow from rocket-engine of lunar explorer on the lunar surface, Master thesis, 1992, School of Engineering, Nagoya University.
11) Boyd, I.D.: Vectorization of a Monte Carlo simulation scheme for nonequilibrium gas dynamics, J. Compu. Phys., Vol.96 (1991), pp.411–427.
12) Sinha, R. Zakkay, V. and Erdos, J.: Flowfield analysis of plume of two-dimensional underexpanded jets by a time-dependent method, AIAA J., Vol.9, No.12 (1971), pp.2363–2369.
13) Poreh, M., Tsuei, Y.G., and Cermak, J.E.: Investigation of a turbulent radial wall jet, J. Appl. Mech. (Trans. ASME), June (1967), pp.457–463.